

Interaction between Non-Heme Iron of Lipoxygenases and Cumene Hydroperoxide: Basis for Enzyme Activation, Inactivation, and Inhibition

Ardeshir Vahedi-Faridi, Pierre-Alexandre Brault, Priya Shah, Yong-Wah Kim, William R. Dunham, and Max O. Funk, Jr.*

Contribution from the Departments of Chemistry and Medicinal and Biological Chemistry, University of Toledo, 2801 West Bancroft Street, Toledo, Ohio 43606

Received October 16, 2003; E-mail: mfunk@utnet.utoledo.edu

Abstract: Lipoxygenase catalysis depends in a critical fashion on the redox properties of a unique mononuclear non-heme iron cofactor. The isolated enzyme contains predominantly, if not exclusively, iron(II), but the catalytically active form of the enzyme has iron(III). The activating oxidation of the iron takes place in a reaction with the hydroperoxide product of the catalyzed reaction. In a second peroxide-dependent process, lipoxygenases are also inactivated. To examine the redox activation/inactivation dichotomy in lipoxygenase chemistry, the interaction between lipoxygenase-1 (and -3) and cumene hydroperoxide was investigated. Cumene hydroperoxide was a reversible inhibitor of the reaction catalyzed by lipoxygenase-1 under standard assay conditions at high substrate concentrations. Reconciliation of the data with the currently held kinetic mechanism requires simultaneous binding of substrate and peroxide. The enzyme also was both oxidized and largely inactivated in a reaction with the peroxide in the absence of substrate. The consequences of this reaction for the enzyme included the hydroxylation at C β of two amino acid side chains in the vicinity of the cofactor, Trp and Leu. The modifications were identified by mass spectrometry and X-ray crystallography. The peroxide-induced oxidation of iron was also accompanied by a subtle rearrangement in the coordination sphere of the non-heme iron atom. Since the enzyme retains catalytic activity, albeit diminished, after treatment with cumene hydroperoxide, the structure of the iron site may reflect the catalytically relevant form of the cofactor.

Introduction

Lipoxygenases constitute an important facet of polyunsaturated fatty acid metabolism in both plants and animals. The products of the reactions catalyzed by these enzymes are intermediates in the biosynthesis of numerous compounds in physiological signaling pathways. For example, in plants lipoxygenase inaugurates the wound-induced biosynthesis of the plant growth hormone jasmonic acid.¹ Arachidonic acid metabolism in animals is governed by cyclooxygenases and lipoxygenases. The eicosanoid products of the lipoxygenase pathway include the leukotrienes, a family of paracrine hormones.² Blocking the lipoxygenase pathway for therapeutic benefit in diseases such as asthma, atherosclerosis, and cancer is an active area of investigation.³

The lipoxygenases catalyze the regio- and stereoselective peroxygenation of the methylene-interrupted unsaturated systems found in natural substrates such as linoleic, linolenic, and arachidonic acids. Remarkably, the products of the catalyzed reaction are conjugated hydroperoxides, compounds with cytotoxic properties.⁴ Therefore, the regulatory properties of the enzyme have important physiological consequences. The reaction catalyzed by lipoxygenases depends in a critical fashion

on the presence of a unique non-heme iron cofactor.⁵ The active form of the enzyme contains iron(III). In the currently held mechanistic hypothesis, the enzyme abstracts hydrogen from the substrate in a step that has the properties of a hydrogen-tunneling reaction.⁶ The electron from a substrate C–H bond reduces the iron, while the proton is taken up by an iron-bound hydroxide. An intermediate free radical combines with molecular oxygen to produce a conjugated peroxy radical which reoxidizes the iron and becomes protonated in the formation of product. Redox cycling of the iron atom during catalysis is firmly established.⁷ However, the enzyme as it is isolated, for example, from soybeans, contains predominantly if not exclusively iron(II).⁸ The only known oxidizing agent for lipoxygenase iron is the hydroperoxide product of its reaction, making kinetic time courses appear highly autocatalytic in nature.⁹

Under certain circumstances, lipoxygenases are sensitive to inactivation by fatty acid hydroperoxides, a self-inactivation reaction.¹⁰ Lipoxygenases are also inactivated by acetylenic

(1) Feussner, I.; Wasternack, C. *Annu. Rev. Plant. Biol.* **2002**, *53*, 275–297.
(2) Funk, C. D. *Science* **2001**, *294*, 1871–1875.
(3) Julemont, F.; Dogne, J. M.; Laeckmann, D.; Pirotte, B.; DeLeval, X. *Expert Opin. Ther. Pat.* **2003**, *13*, 1–13.

(4) Schneider, C.; Tallman, K. A.; Porter, N. A.; Brash, A. R. *J. Biol. Chem.* **2001**, *276*, 20831–20838.
(5) Solomon, E. I.; Brunold, T. C.; Davis, M. I.; Kemsley, J. N.; Lee, S. K.; Lehnert, N.; Neese, F.; Skulan, A. J.; Yang, Y. S.; Zhou, J. *Chem. Rev.* **2000**, *100*, 235–349.
(6) Knapp, M. J.; Rickert, K.; Klinman, J. P. *J. Am. Chem. Soc.* **2002**, *124*, 3865–3874.
(7) Funk, M. O.; Carroll, R. T.; Thompson, J. F.; Sands, R. H.; Dunham, W. R. *J. Am. Chem. Soc.* **1990**, *112*, 5375–5376.
(8) Dunham, W. R.; Carroll, R. T.; Thompson, J. F.; Sands, R. H.; Funk, M. O. *Eur. J. Biochem.* **1990**, *190*, 611–617.

analogues of their substrates.¹¹ In this instance, inactivation was accompanied by conversion of a specific methionine residue in the enzyme to methionine sulfoxide. The hypothesis was that the acetylenic analogues were oxygenated to a reactive intermediate allenic hydroperoxide that could subsequently oxidize methionine, resulting in inactivation. Support for the link between sulfoxide formation and inactivation, however, has not been found. For example, the turnover-dependent inactivation of leukocyte 12-lipoxygenase was not significantly altered in any of three engineered proteins where the sulfides in candidate methionines were replaced by the less reactive aliphatic amino acid side chains of leucine or valine in site-directed mutagenesis experiments.¹²

Understanding the activation/inactivation chemistry of lipoxygenases is important since this could provide a means for controlling catalysis, both in the laboratory and for therapeutic purposes. For example, compounds that inhibit lipoxygenase by interfering with the oxidation/activation reaction have recently been discovered.¹³ To provide a basic understanding of the chemistry underlying the activation and inactivation of lipoxygenases by peroxides, we present the results of a study of the interaction of soybean lipoxygenases with cumene hydroperoxide. Lipoxygenase-1 was *oxidized* and largely *inactivated* by this compound. We offer EPR spectroscopic, mass spectrometric, and crystallographic evidence for the chemistry that accounts for these effects. Because the enzyme retains significant catalytic activity following treatment with cumene hydroperoxide and the EPR spectroscopic features of the treated enzyme are identical to the product activated enzyme, the iron site in the cumene hydroperoxide treated enzyme may correspond to the active iron(III) form of the cofactor. Cumene hydroperoxide was also an inhibitor of the steady-state phase of the catalyzed reaction, but remarkably only at very high substrate concentration.

Results and Discussion

Cumene Hydroperoxide Is an Inhibitor of the Steady-State Phase of Lipoxygenase Catalysis. When cumene hydroperoxide was included in substrate solutions at various concentrations under standard assay conditions (enzyme added last), a distinctive pattern of inhibition of the steady-state phase of the reaction was observed. At low substrate concentration, there was a small effect of the presence of cumene hydroperoxide on the rate of the catalyzed reaction. At higher concentrations of substrate, however, there was a major reduction in the rate even at relatively low concentrations of the peroxide (<20 μM). The lipoxygenase-1-catalyzed oxygenation of linoleic acid has interesting and unusual characteristics, e.g., product activation and substrate inhibition. All of the features of the kinetics have been accommodated by a mechanism that invokes a single substrate binding site and two forms of the enzyme depending upon the oxidation state of the cofactor iron (II or III).¹⁴ A nonlinear least-squares regression analysis of the maximum rate

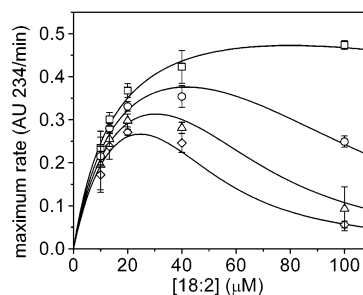


Figure 1. Effect of cumene hydroperoxide on the steady-state (maximum rate) phase of the lipoxygenase-1-catalyzed reaction. Substrate, linoleic acid; pH, 9.0; temperature, 25.0 °C. The solid lines represent the fit of the kinetic mechanism to the experimental values. [Cumene hydroperoxide]: squares, none; circles, 5 μM ; triangles, 10 μM ; diamonds, 15 μM .

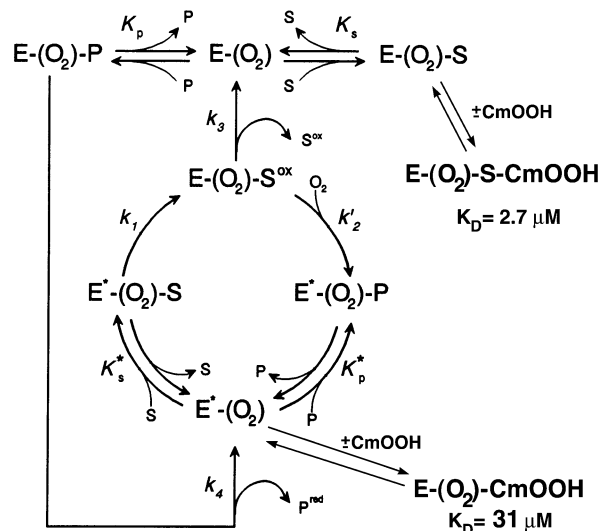


Figure 2. Kinetic mechanism for lipoxygenase catalysis from Schilstra et al.¹⁴ including terms for cumene hydroperoxide (CmOOH) that account for the inhibition observed in Figure 1.

data with this molecular mechanism was conducted.¹⁵ A reasonable agreement with the data (Figure 1) was obtained by allowing for cumene hydroperoxide binding to the iron(III) enzyme ($K_D = 31 \mu\text{M}$) to account for the modest inhibition observed at low substrate concentration and more importantly to the iron(II) enzyme–substrate complex to simulate the inhibitory effect of the hydroperoxide at high substrate concentration ($K_D = 2.7 \mu\text{M}$). The kinetic mechanism derived by Schilstra et al.¹⁴ is reproduced in Figure 2 along with the terms accounting for cumene hydroperoxide inhibition. The analysis employed values for the various rate and equilibrium constants (eight parameters) that are consistent with the literature on this subject.¹⁶

The fitting procedure predicts association of lipoxygenase-1 with cumene hydroperoxide in both the free form and with a substrate molecule bound to the iron(II) form. Including terms for cumene hydroperoxide interactions with any of the other forms of the enzyme did not account for the inhibitory effect or improve the fit. For example, terms for the hydroperoxide binding either to the iron(III)–substrate complex or the free iron(II) form alone could not account for the extreme sensitivity

(9) Schilstra, M. J.; Veldink, G. A.; Vliegthart, J. F. G. *Biochemistry* **1993**, *32*, 7686–7691.

(10) Hartel, B.; Ludwig, P.; Schewe, T.; Rapoport, S. M. *Eur. J. Biochem.* **1982**, *126*, 353–357.

(11) Nieuwenhuizen, W. F.; Van der Kerk-Van Hoof, A.; van Lenthe, J. H.; Schaik, R. C. V.; Versluis, K.; Veldink, G. A.; Vliegthart, J. F. G. *Biochemistry* **1997**, *36*, 4480–4488.

(12) Richards, K. M.; Marnett, L. J. *Biochemistry* **1997**, *36*, 6692–6699.

(13) Moody, J. S.; Marnett, L. J. *Biochemistry* **2002**, *42*, 10297–10303.

(14) Schilstra, M. J.; Veldink, G. A.; Verhagen, J.; Vliegthart, J. F. G. *Biochemistry* **1992**, *31*, 7692–7699.

(15) Kuzmic, P. *Anal. Biochem.* **1996**, *237*, 260–273.

(16) Schilstra, M. J.; Veldink, G. A.; Vliegthart, J. F. G. *Biochemistry* **1994**, *33*, 3974–3979.

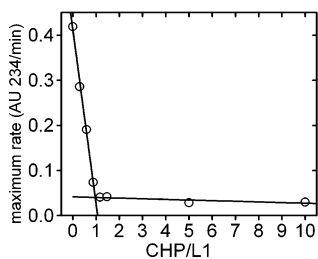


Figure 3. Effect of preincubation of cumene hydroperoxide on the steady-state (maximum rate) phase of the lipoxygenase-1-catalyzed reaction. Lipoxygenase-1 (0.5 μM) treated with the indicated ratio of cumene hydroperoxide in sodium borate buffer (0.1 M, pH 9.0, 25 $^{\circ}\text{C}$) was subsequently combined with substrate (linoleic acid, 100 μM , 0.1 M sodium borate buffer, pH 9.0, 25.0 $^{\circ}\text{C}$) for the rate determination.

of the rate to the presence of the hydroperoxide at high substrate concentration. Further, including steps involving the iron(III) enzyme–substrate complex and the peroxide did not improve the agreement between the kinetic mechanism and the data.

There is mounting evidence that lipoxygenase is capable of binding multiple molecules, and the kinetic data presented here certainly support those findings. For example, a distinctive pattern of inhibition of the steady-state phase of lipoxygenase-1 catalysis by oleyl sulfate was consistent with binding at an allosteric site.¹⁷ This finding was confirmed and extended when it was recently discovered that oleyl sulfate does not inhibit lipoxygenase-1 activation by the hydroperoxide product of its catalyzed reaction but is exclusively an allosteric inhibitor of turnover.¹⁸ The kinetic data for lipoxygenase-1 in the presence of cumene hydroperoxide are also consistent with simultaneous binding of two molecules by the protein.

In the Absence of Substrate, Cumene Hydroperoxide Is an Efficient Inactivator of Lipoxygenase-1. Preincubation of cumene hydroperoxide with lipoxygenase-1 prior to initiation of the catalyzed reaction under standard assay conditions led to a nearly complete loss of catalytic activity. The stoichiometry of the inactivation is illustrated in Figure 3 for lipoxygenase-1 present in the preincubation mixture at a concentration of 0.25 μM . The drastic reduction in catalytic efficiency caused by

Table 1. Thermochemical Properties of the Reactions between Lipoxygenase-1 and Cumene Hydroperoxide and 13-HPOD from Isothermal Titration Calorimetry

calorimeter parameters	lipoxygenase-1 + 13-HPOD	lipoxygenase-1 + cumene hydroperoxide
stoichiometry (N)	1.07 ± 0.12	1.00 ± 0.07
equilibrium constant (K)	$1.5 \pm 0.9 \times 10^8$	$7.6 \pm 1.0 \times 10^7$
ΔH (kcal/mol)	-84.2 ± 3.2	-114 ± 2.6
ΔS (cal/deg-mol)	-241 ± 11	-340 ± 8
ΔG (kcal/mol)	-11.2 ± 0.3	-11.1 ± 0.2

^a Error is reported as the standard deviation of three separate determinations.

cumene hydroperoxide corresponds to an interaction at a one-to-one ratio. The reaction takes place at a rapid rate since there was no indication of an incomplete process during the time required (seconds) to mix the reagents (at low micromolar concentrations) and initiate the assay. While the activity declines by greater than 90% relative to an untreated control, it is also apparent that the residual activity of the enzyme was not zero.

The reaction between lipoxygenase-1 and cumene hydroperoxide was characterized by isothermal titration calorimetry. For reference purposes, the enzyme–product (*Z,E*-13(*S*)-hydroperoxy-9*Z*,11*E*-octadecadienoic acid, 13-HPOD) interaction was measured under the same conditions. Representative titration experiments for the reaction of each of the hydroperoxides with lipoxygenase-1 are presented in Figure 4, and the corresponding calorimetric values are collected in Table 1. It is apparent that both peroxides participate in reactions with the enzyme that display unit stoichiometry and are very exothermic. However, the favorable enthalpy change is also opposed by a large unfavorable entropy change in each experiment. The magnitudes of the enthalpy changes are much larger than what is typically observed for simple ligand-binding interactions.¹⁹ The reaction between 13-HPOD and lipoxygenase-1 is known to involve oxidation of the active-site iron atom, and this redox chemistry must contribute to the thermodynamic parameters for that determination.²⁰ The Gibbs free energy calculated from measurements and estimates of standard reduction potentials

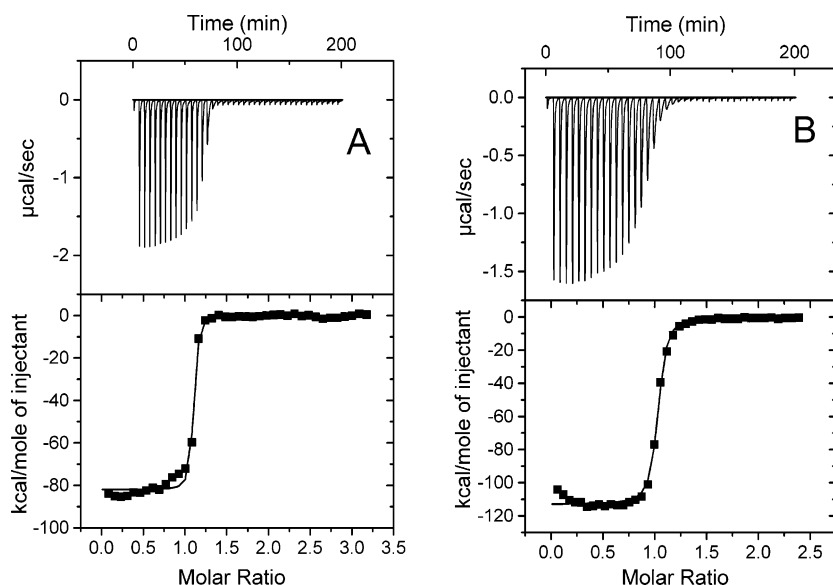


Figure 4. Examples of isothermal titration calorimetry for the reaction between lipoxygenase-1 and cumene hydroperoxide (A) and 13-HPOD (B). The enzyme was in the cell (0.008 mM, 1.43 mL) in 0.1 M Tris HCl, pH 8.5 at 30.0 $^{\circ}\text{C}$ and was titrated (0.01 mL injections) with the peroxides (0.100 mM) in the same buffer.

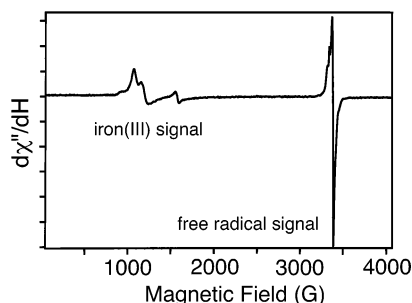
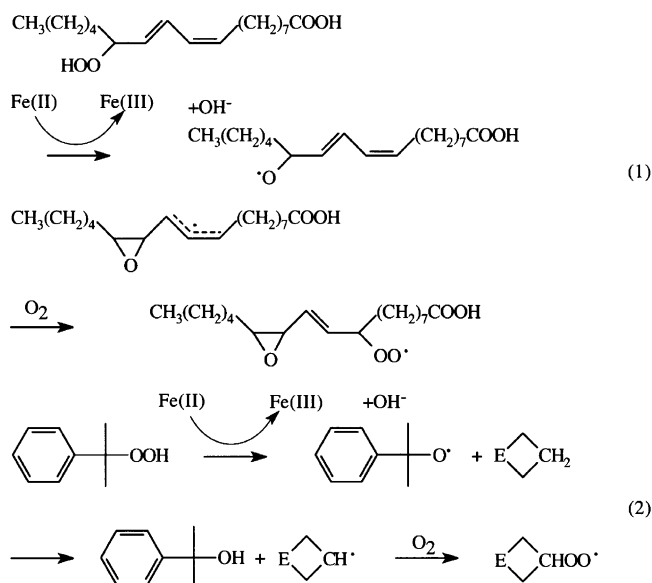


Figure 5. EPR spectroscopy (9 GHz) for lipoygenase-1 treated with cumene hydroperoxide. Lipoygenase-1 (213.5 μ M, 0.1 M TrisHCl, pH 7.0) treated with cumene hydroperoxide (427 μ M). Spectral conditions: microwave power, 5 mW; field modulation, 1 mT; temperature, 25 K.

for the redox reactions account reasonably well for the value obtained in the microcalorimetry experiments. For example, Nelson estimated the reduction potential for lipoygenase Fe(II)/Fe(III) to be 0.6 ± 0.1 V (vs NHE) on the basis of reactivity toward a series of catechols.²¹ The measured electrode potential for cumene hydroperoxide in aqueous solution is 0.23 V (vs NHE).²² This gives an expected free energy change of -8.9 ± 2.4 kcal/mol, which is within experimental error of the thermochemical value, -11.1 ± 0.2 kcal/mol. The similarity in the thermodynamic parameters for the interaction between the two peroxides and lipoygenase-1 led to the hypothesis that the two reactions shared common elements, although one compound activates the enzyme while the other inactivates it.

Evidence for the oxidation of lipoygenase-1 iron by cumene hydroperoxide was sought using EPR spectroscopy. Samples of lipoygenase-1 treated with cumene hydroperoxide in varying ratios (1:1, 2:1, 5:1, and 10:1) were transferred to EPR tubes. Measurements were conducted at 25 K. A representative example from the collection of EPR spectra is presented in Figure 5. All of the spectra had the same characteristics and signal intensities, i.e., the ratio of cumene hydroperoxide to lipoygenase-1 beyond 1:1 was not an influential factor. Each spectrum had contributions from two signals. The low-field signal ($g = 6$) is the same as the signal in spectra for the high-spin iron(III) form of lipoygenase-1 obtained when the native enzyme is treated with 13-HPOD, providing evidence that cumene hydroperoxide oxidizes the cofactor.²³ The high-field signal ($g = 2$) can be attributed to free radical species. Free radical EPR signals in lipoygenase-1 samples treated with 13-HPOD or linoleic acid/oxygen have been characterized previously.²⁴ Depending on the conditions of the experiment, either alkyl or peroxy radicals derived from linoleic acid were observed. The free radical signals obtained from cumene hydroperoxide treated samples most closely resemble the peroxy radical signals. However, because there was no linoleic acid present and cumene hydroperoxide would not be expected to produce peroxy radicals in a reaction with iron(II), the signals

are most likely to be due to a radical species on the enzyme. The formation of peroxy radicals in alternate ways, via β -scission and combination of alkyl radicals with oxygen or through bimolecular reactions with cumene hydroperoxide, cannot be ruled out. There is indirect evidence that when 13-HPOD reacts with lipoygenase-1, electron transfer from iron(II) produces the alkoxy radical. For example, the products of the reaction include epoxides formed as a consequence of internal rearrangement (eq 1).²⁵ By analogy, the oxidation of lipoygenase iron by cumene hydroperoxide would form the corresponding cumyloxy radical (eq 2). However, this species would be incapable of rearrangement and combination with oxygen. Alternatively the radical could perform hydrogen-atom abstraction from nearby amino acid side chains. The alkyl radicals formed in this way could combine with molecular oxygen, a molecule with access to the active site as a substrate in the catalyzed reaction, to form peroxy radicals.



Reaction between Cumene Hydroperoxide and Lipoygenase-1 Results in Chemical Modification of Active Site Residues.

The outcome of the reaction between the enzyme and cumene hydroperoxide was explored using mass spectrometry and X-ray crystallography. Samples of lipoygenase-1 either treated or not treated with cumene hydroperoxide were reduced and carboxymethylated and digested with trypsin. The samples were analyzed by HPLC-ES/MS/MS. Total ion current chromatograms for the cumene hydroperoxide treated and untreated enzyme were nearly identical. The digestion experiments with and without cumene hydroperoxide treatment were conducted twice with exactly the same results. Careful examination of the chromatograms and the underlying mass spectra revealed two significant differences between the treated and untreated samples. One change that took place as a result of cumene hydroperoxide treatment was the appearance in the chromatograms of an $M - 2\text{H}^{2+}$ species with m/z 982 (Figure 6, right side). The appearance of the peptide giving rise to this ion was coincident with the loss of signal for an $M - 2\text{H}^{2+}$ species with m/z 974 (Figure 6, left side). The difference between the two ions corresponds to the addition of one oxygen atom to the

(17) Mogul, R.; Holman, T. R. *Biochemistry* **2001**, *40*, 4391–4397.

(18) Ruddat, V. C.; Whitman, S.; Holman, T. R.; Bernasconi, C. F. *Biochemistry* **2003**, *42*, 4172–4178.

(19) Leavitt, S.; Freire, E. *Curr. Opin. Struct. Biol.* **2001**, *11*, 560–566.

(20) De Groot, J. J. M. C.; Veldink, G. A.; Vliegthart, J. F. G.; Boldingh, J. Wever, R.; Van Gelder, B. F. *Biochim. Biophys. Acta* **1975**, *377*, 71–79.

(21) Nelson, M. J. *Biochemistry* **1988**, *27*, 4273–4278.

(22) Willits, C. O.; Ricciuti, C.; Knight, H. B.; Swern, D. *Anal. Chem.* **1952**, *24*, 785–790.

(23) Slappendel, S.; Aasa, R.; Malmstrom, B. G.; Verhagen, J.; Veldink, G. A.; Vliegthart, J. F. G. *Biochim. Biophys. Acta* **1982**, *708*, 259–265.

(24) Nelson, M. J.; Cowling, R. A.; Seitz, S. P. *Biochemistry* **1994**, *33*, 4966–4973.

(25) Garssen, G. J.; Veldink, G. A.; Vliegthart, J. F. G.; Boldingh, J. *Eur. J. Biochem.* **1976**, *62*, 33–36.

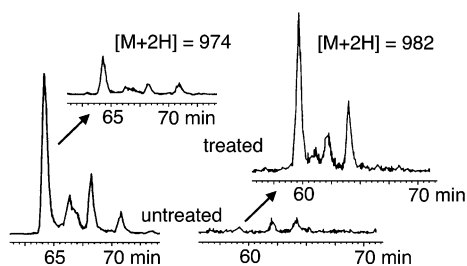


Figure 6. Mass chromatograms for $M - 2H^{2+}$ ions at m/e 974 and 982. Lipoxygenase-1 treated (right) with excess cumene hydroperoxide (1.4X); reduced, carboxymethylated, and trypsinized; resolved by RP-HPLC (C18); electrospray ionization mass spectrometry. Control: replicate not including cumene hydroperoxide treatment (left).

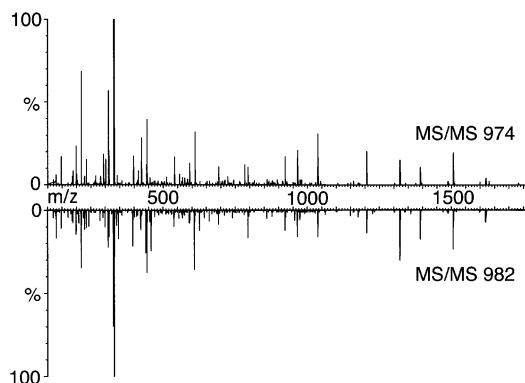


Figure 7. CID mass spectra for $M - 2H^{2+}$ ions at m/e 974 and 982 in the mass chromatograms.

peptide, the consequence of an oxygen insertion or hydroxylation reaction. The peptide in the untreated sample providing the $M - 2H^{2+}$ ion with m/z 974 was readily identified by a standard database matching program based on the raw data as the peptide 544–561 (QSLINANGIIEITFLPSK) in the lipoxygenase-1 sequence. The mass spectrometer conducted MS/MS determinations on the ion with m/z 974 a total of 10 times during the analysis of the two samples with the same peptide identified on the basis of its fragmentation pattern each time.

When the MS/MS data for each of the $M - 2H^{2+}$ ions 974 and 982 were compared (Figure 7), the fragmentation patterns in the two spectra were nearly the same. For example, there was a family of y -type ions in both spectra from $y_1 \rightarrow y_{15}$, indicating that the modification causing the overall mass difference was present in the three N-terminal amino acids: QSL. There were b -type ions in both mass spectra for the first two amino acids b_1 , m/z 129 and b_2 , m/z 216. However, for b_3 , m/z 329 there was an ion present in the untreated sample that was not present in the cumene hydroperoxide treated sample. Conversely, there was an ion present at m/z 345 in the treated sample ($b_3 + O$) that was not present in the untreated sample. These findings were consistent with the equivalent of an oxygen insertion reaction (hydroxylation) at Leu-546 in lipoxygenase-1 upon treatment with cumene hydroperoxide. The side chain for Leu-546 is adjacent to the iron atom in the active site in the crystallographically determined three-dimensional structure of lipoxygenase-1.²⁶

A second difference between the cumene hydroperoxide treated and untreated samples of lipoxygenase-1 was also

identified using mass spectrometry. A signal for an $M - 3H^{3+}$ ion with m/z 1304.57 in the untreated samples declined in intensity along with the appearance of a new $M - 3H^{3+}$ peak intensity with m/z 1309.89. The ion in the untreated sample had the proper mass for the peptide from 484 to 516 in lipoxygenase-1; 3910.68 obsd vs 3910.85 calcd for the neutral carboxamidomethylated peptides. MS/MS conducted on the 1304.57 ion produced a significant match for the ions expected for fragmentation at the ends of the peptide: b -type, six matching ions and y -type eight matching ions. The ion in the cumene hydroperoxide treated samples had the correct mass for the same peptide with the addition of a single oxygen atom; 3926.64 obsd vs 3926.84 calcd for the neutral carboxamidomethylated peptides. Due to its relatively low intensity, the mass spectrometer did not select the 1309.89 ion for MS/MS determination. The observations of these changes in the mass spectra suggested that an oxygen insertion in 484–516 also took place. This peptide is located in the enzyme active site. For example, it contains two of the three histidine residues, His-499 and His-504, that act as ligands to the iron.²⁶

Crystals of lipoxygenase-3 were treated with a cumene hydroperoxide solution for 12–24 h. The crystals were gradually transferred to a solution containing the cryoprotectant glycerol to circumvent a previously observed change in the crystal lattice upon flash freezing.²⁷ X-ray diffraction measurements at 98 K followed by solution of the structure using molecular replacement revealed two (partially) oxygenated amino acid side chains in the neighborhood of the non-heme iron cofactor. As illustrated in Figures 8 and 9, electron density located adjacent to the β -position of Trp-519 (Trp-500 in lipoxygenase-1) was present in the $2Fo - Fc$ electron density map as well as in the $Fo - Fc$ omit map, at contour levels of 2 and 3σ , respectively, consistent with hydroxylation of this residue upon cumene hydroperoxide treatment of the lipoxygenase-3 crystals. This modification accounts for the increase in mass observed for the tryptic peptide for residues 484–516 in cumene hydroperoxide treated lipoxygenase-1 using mass spectrometry. While β -hydroxylation at tryptophan is not common, as the indole ring of the side chain is readily oxidized, there are examples of this chemistry taking place at enzyme active sites. For example, a unique posttranslational modification, autocatalytic formation of β -hydroxylated tryptophan, in the active site of white rot fungus lignin peroxidase has been described.²⁸ Quite remarkably, the hydroxylated enzyme is catalytically active and the observed form in the isolated enzyme. In the crystallographically determined structure of lipoxygenase-3 treated with 13-HPOD, the peroxide forms a complex with the active site iron.²⁹ The polyunsaturated fatty acid binds with its olefin component between Trp-519 and one of the iron ligands, His-518. Hydroxylation at the β -position of Trp-519 would introduce a hydroxyl group directly into this site. The alteration would have deleterious consequences for catalysis either by physically blocking access of polyunsaturated fatty acid molecules to the iron site or by drastically changing the polarity of the binding site. In either case, the hydroxylation at Trp-500 would be

(27) Skrzypczak-Jankun, E.; Bianchet, M. A.; Amzel, L. M.; Funk, M. O. *Acta Crystallogr., Sect. D* **1996**, *52*, 959–965.

(28) Blodig, W.; Smith, A. T.; Doyle, W. A.; Piontek, K. J. *Mol. Biol.* **2001**, *305*, 851–861.

(29) Skrzypczak-Jankun, E.; Bross, R. A.; Carroll, R. T.; Dunham, W. R.; Funk, M. O. *J. Am. Chem. Soc.* **2001**, *123*, 10814–10820.

(26) Minor, W.; Stecko, J.; Otwinowski, Z.; Bolin, J. T.; Walter, R.; Axelrod, B. *Biochemistry* **1996**, *35*, 10687–10701.

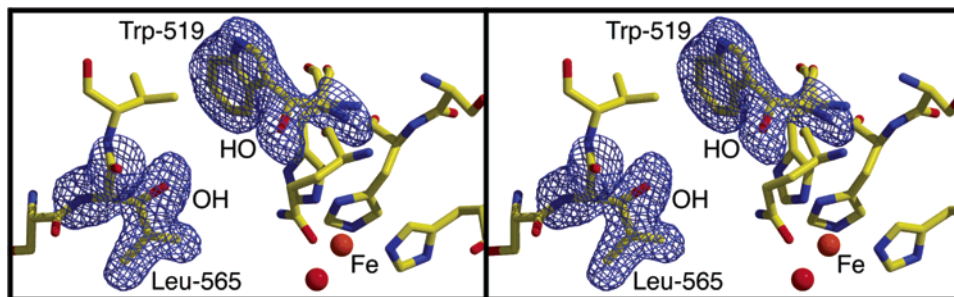


Figure 8. $2F_o - F_c$ electron density map showing $C\beta$ hydroxylation sites at residues Trp-519 and Leu-565 at 2.0 Å resolution in lipoxygenase-3 crystals. The electron density is contoured at 2σ .

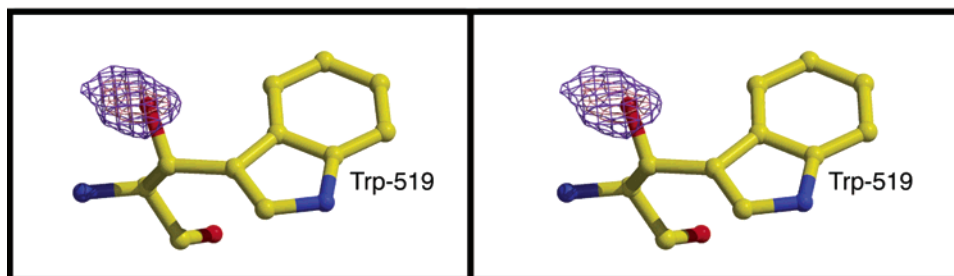


Figure 9. $F_o - F_c$ electron density map showing the $C\beta$ hydroxylation site at residue Trp-519 contoured at 3σ . Only the hydroxyl group was omitted.

expected to be a major contributor to the inactivation of lipoxygenase-1 upon cumene hydroperoxide treatment.

Site-directed mutagenesis studies have not yet been conducted on Trp-500 in lipoxygenase-1. However, this tryptophan is highly conserved upon examination of sequence alignments for plant lipoxygenases, and mutagenesis (to Ala) has been conducted on the corresponding Trp-523 in the pea seed enzyme.³⁰ The genetically modified enzyme had a catalytic efficiency (k_{cat}/K_M) equivalent to 2% of the wild-type enzyme. The experiment was carried out on the pea seed enzyme to modify (enlarge) the substrate binding site for linoleate to see if there would be a change in the overall substrate specificity or a change in the regiochemical outcome of the peroxidation reaction. It is tempting to use this result to rationalize the reduction in catalytic activity we observed in cumene hydroperoxide treated lipoxygenase-1 when Trp-500 was chemically modified. However, there are significant differences between the two experiments. The site-directed mutagenesis experiment brought about a drastic side chain change ($W \rightarrow A$), and while the modified enzyme displayed the characteristic EPR signal for iron(III) lipoxygenase, it had an intensity of only 10% of the wild-type enzyme prepared under identical conditions. Therefore, the modification may have altered the protein structure in the vicinity of the iron site, causing a reduced iron content or creating an enzyme that could not be activated to the iron(III) form. In contrast to the site-directed mutagenesis experiment, the chemical modification by cumene hydroperoxide caused a change toward a more polar environment with additional hydrogen-bonding capacity in the substrate-binding channel. The alteration of tryptophan may account for the decline in catalytic activity seen in the two kinds of experiments, but there could well be different reasons for this outcome in each instance.

Electron density was also found adjacent to the β -position of Leu-565 (Leu-546 in lipoxygenase-1) in the three-dimensional

structure of lipoxygenase-3 crystals treated with cumene hydroperoxide (Figure 8). This change corresponds to the increase in mass for the tryptic peptide for residues 544–561 in lipoxygenase-1 determined by mass spectrometry. The alteration, like the β -hydroxylation of Trp-500, causes a shift to a more polar environment in the substrate-binding channel. Site-directed mutagenesis experiments have been carried out on Leu-546 in lipoxygenase-1.³¹ The objective was to enlarge (Leu \rightarrow Ala) the substrate binding site in the vicinity of the cofactor iron site to see if this would change the regiochemical or stereochemical outcome of catalysis. The genetically modified enzyme had a catalytic efficiency (k_{cat}/K_M) that was approximately 10% of the value for the wild-type enzyme. This reduction in catalytic activity has the same magnitude that was observed for the reaction with cumene hydroperoxide, but as before, the alterations are also significantly different.

The Cofactor in Cumene Hydroperoxide Treated Lipoxygenase May Represent the Essential Iron(III) of Catalysis.

Crystals of the catalytically active iron(III) form of lipoxygenases for X-ray diffraction analysis have been difficult to obtain. Solutions of the enzyme oxidized in a one-to-one ratio with product are readily produced. However, crystals obtained from concentrated solutions prepared in this fashion are not significantly different from the native iron(II) enzyme. The reason for this is not entirely clear, but it has been reported that very concentrated solutions (> 1 mM) of lipoxygenase-1 treated with an equimolar amount of 13-HPOD have proportionately less EPR visible iron than less concentrated solutions (250 μ M).³² This “spontaneous reduction” of the iron(III) in lipoxygenase-1 was also observed during prolonged storage of solutions.²³ The reversion of the iron(III) enzyme to the native form under the high-concentration conditions required for crystallization could

(30) Hughes, R. K.; Lawson, D. M.; Hornostaj, A. R.; Fairhurst, S. A.; Casey, R. *Eur. J. Biochem.* **2001**, *268*, 1030–1040.

(31) Knapp, M. J.; Seebeck, F. P.; Klinman, J. P. *J. Am. Chem. Soc.* **2001**, *123*, 2931–2932.

(32) Petersson, L.; Slappendel, S.; Feiters, M. C.; Vliegthart, J. F. G. *Biochim. Biophys. Acta* **1987**, *913*, 228–237.

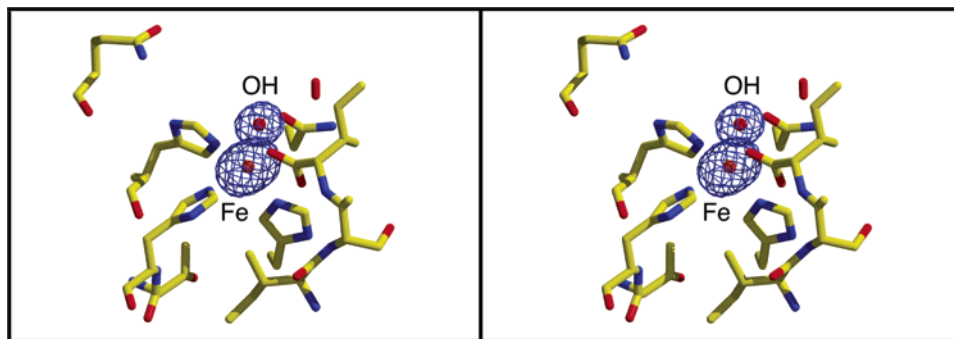


Figure 10. $F_o - F_c$ electron density map showing spherical electron density centered at 2.05 Å for the iron atom. The electron density is contoured at 3σ .

Table 2. Bond Distances and Angles for the Non-Heme Iron Sites in the Three-Dimensional Structures of Soybean Lipoxigenases Determined by X-ray Crystallography

	lipoxigenase-3, CmOOH 98 K	lipoxigenase-1 100 K ²⁶	lipoxigenase-3 RT ³⁴	lipoxigenase-3, 13-HPOD RT ²⁹
bond distances (Å)				
Fe–His-518 (NE2)	2.37	2.21/2.24	2.23	2.23
Fe–His-523 (NE2)	2.38	2.34	2.21	2.24
Fe–His-709 (NE2)	2.41	2.29	2.26	2.28
Fe–Asn-713 (OD1)	3.33	2.87	3.01	2.28
Fe–Ile-857 (OXT)	2.79	2.28	2.13	2.05
Fe–Ile-857 (O)	2.39	3.51	3.01	3.07
Fe–O22/OH	2.05	2.11	4.02	2.01
bond angles (deg)				
His-518 (NE2)–Fe–His-523 (NE2)	93.8	94.0	91.6	84.5
His-518 (NE2)–Fe–His-709 (NE2)	108.2	99.7	100.7	98.9
His-518 (NE2)–Fe–Asn-713 (OD1)	68.8	74.5	67.8	77.9
His-518 (NE2)–Fe–Ile-857 (OXT)	158.1	166.6	171.6	178.2
His-518 (NE2)–Fe–Ile-857 (O)	135.8	133.7	127.9	133.7
His-518 (NE2)–Fe–O22/OH	85.7	89.0	76.8	90.1
His-523 (NE2)–Fe–His-709 (NE2)	109.7	100.6	86.5	89.2
His-523 (NE2)–Fe–Asn-713 (OD1)	159.9	164.1	158.6	161.5
His-523 (NE2)–Fe–Ile-857 (OXT)	108.1	97.0	94.5	94.3
His-523 (NE2)–Fe–Ile-857 (O)	91.4	94.5	110.2	107.5
His-523 (NE2)–Fe–O22/OH	118.4	99.5	69.4	82.7
His-709 (NE2)–Fe–Asn-713 (OD1)	86.2	92.3	91.5	87.9
His-709 (NE2)–Fe–Ile-857 (OXT)	63.4	85.6	85.5	82.4
His-709 (NE2)–Fe–Ile-857 (O)	111.2	123.1	126.4	125.1
His-709 (NE2)–Fe–O22/OH	128.9	157.4	155.6	167.3
Asn-713 (OD1)–Fe–O22/OH	52.5	69.8	109.3	102.9
Ile-857 (OXT)–Fe–Asn-713 (OD1)	90.0	93.2	106.6	103.4
Ile-857 (OXT)–Fe–O22/OH	85.4	81.8	99.9	88.4
Ile-857 (O)–Fe–Asn-713 (OD1)	94.4	93.2	88.0	89.0
Ile-857 (O)–Fe–O22/OH	53.9	44.7	68.6	49.5

^a Lipoxigenase-1 equivalent residues: His-499, His-504, His-690, Asn-694, and Ile-839.

account for the fact that crystals of the oxidized enzyme have been difficult to prepare.

When preexisting crystals of lipoxigenase-3 were treated with cumene hydroperoxide and analyzed crystallographically, in addition to the oxidative modifications already described, a subtle rearrangement was observed in the coordination sphere of the iron atom relative to the native state. The new geometry is illustrated in Figure 10, and the bond distances and angles for the iron site are collected in Table 2. Values of angles and distances for other crystallographically determined lipoxigenase structures were included in the table for comparison purposes. The iron in the treated crystals was five-coordinate including three nitrogen ligands contributed by histidines and one oxygen ligand from the C-terminal isoleucine, usual features for lipoxigenase iron. Despite certain specific differences, the geometry closely resembles the one in the low-temperature structure of native lipoxigenase-1. For example, a superposition analysis for the iron and its six nearest neighboring atoms (His-

518 NE2, His-523 NE2, His-709 NE2, Ile-857 O/OXT, Asn-713 OD1, and OH) resulted in an rms deviation of 0.39 Å. The orientation of the coordinating C-terminal carboxylate group of Ile-857 was, however, significantly different in the iron environment for the protein in the cumene hydroperoxide treated crystals. Whereas the carboxylates in the native enzyme and the 13-HPOD product complex employ the oxygen atom designated OXT for iron coordination, the cumene hydroperoxide treated enzyme uses the oxygen atom designated O. While the two oxygen atoms may be chemically equivalent, they have distinguishable orientations in the three-dimensional structures. Also, the position of Asn-713 was beyond a bonding distance as was found for the structures of the native enzymes. In the 13-HPOD complex with lipoxigenase-3, Asn-713 becomes an iron ligand. The fifth ligand to iron in the cumene hydroperoxide treated crystals was a solvent molecule or hydroxide ion. There was spherical electron density in the $2F_o - F_c$ and the $F_o - F_c$ omit map (contour levels 3σ) centered at 2.05 Å from the iron

(Figure 10). This value is consistent with the bond distance expected for iron(III) hydroxide. The 19 appropriate compounds in the Cambridge Crystallographic Data Base have an average iron(III) hydroxide bond distance of $1.96 \pm 0.10 \text{ \AA}$. The best analogy in a non-heme protein is iron(III) superoxide dismutase. The average iron hydroxide bond distance in the five crystallographically determined structures is $2.16 \pm 0.18 \text{ \AA}$.³³ The current hypothesis for the mechanism of lipoxygenase catalysis invokes hydrogen abstraction from the substrate in a reaction that has the properties of hydrogen tunneling.⁶ In the process, the electron reduces the iron and the proton is thought to combine with iron-bound hydroxide. There is spectroscopic evidence for the existence of the iron hydroxide,³⁴ and water molecules were found in the vicinity of the iron in the three-dimensional structures of the native, iron(II) lipoxygenases: at 4.0 \AA in lipoxygenase-3 at room temperature and at 2.01 \AA in lipoxygenase-1 at 100 K .^{25,35} The structure reported here confirms the existence of iron hydroxide in the peroxide oxidized form of the enzyme.

The five-coordinate iron site in the cumene hydroperoxide treated lipoxygenase-3 crystals is also remarkably similar to the iron environment found in *E. coli* galactose-1-phosphate uridylyltransferase, which was described as a distorted square pyramidal geometry.³⁶ A superposition analysis of the three histidine nitrogen atoms and two oxygen atoms in the coordination spheres for the two enzymes resulted in an rms deviation of 0.44 \AA . In contrast to the situation in lipoxygenase-3, the sharp bond angle in the coordination sphere of iron in galactose-1-phosphate uridylyltransferase is achieved through bidentate ligation of the side chain of a glutamate residue. Remarkably, the iron in galactose-1-phosphate uridylyltransferase was not involved in catalysis.³⁷ Compounds with an iron configuration similar to the one found in the cumene hydroperoxide treated lipoxygenase-3 crystals have been produced previously in model studies for the mononuclear non-heme iron sites in various metalloproteins including lipoxygenase. For example, monomeric five-coordinate complexes were obtained for iron(II) with a tris-(pyrazolyl)borate and various acetate and benzoate ligands.³⁸ The geometry was described as either square pyramidal or trigonal bipyramidal depending on the exact combination of ligands. The best models for the spectroscopic and chemical properties of the lipoxygenase iron site have all been six-coordinate distorted octahedral complexes.^{39–41} It may be difficult to produce model complexes absent a protein scaffolding with the same level of distortion from ideal geometry as observed in the iron site of the cumene hydroperoxide treated crystals of lipoxygenase-3.

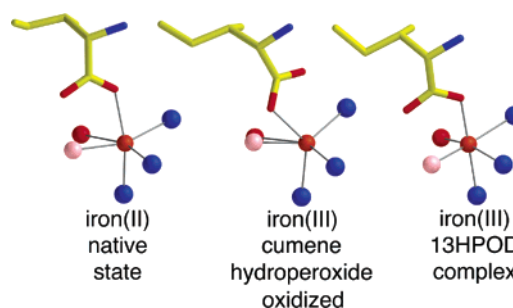


Figure 11. Schematic representation of the iron sites in three crystallographically determined three-dimensional structures of lipoxygenase. Blue spheres, His N; orange sphere, Fe; red sphere, Asn O; pink sphere, OH or 13-HPOD O; structure, C-terminal Ile.

Because lipoxygenase-1 retains residual catalytic activity after treatment with cumene hydroperoxide, it is reasonable to suppose that the iron site in the treated crystals reflects the situation in the active enzyme and that the observed coordination geometry is a feature of the activated complex during catalysis. To illustrate the changes that could be taking place during catalysis, three schematic representations of the iron sites from the same perspective at various stages of the catalyzed reaction (native \rightarrow peroxide oxidized \rightarrow product complex) are presented in Figure 11. Significantly, treatment with cumene hydroperoxide resulted in an increase in the degree of iron atom exposure to the space where fatty acid binding takes place, as the bond angle His-523/Fe/OH expanded to almost 120° . This feature might have important consequences for the catalyzed reaction. Because of the mass of the proton, hydrogen tunneling can account for reactions taking place over only a limited distance ($0.6\text{--}0.7 \text{ \AA}$).⁴² The rearrangement that takes place in the lipoxygenase iron site upon peroxide-induced oxidation allows for close approach of the substrate to the cofactor. Other attributes of the iron site remain to be reconciled with the observed structure. For example, existing evidence implicates a relatively high redox potential for the cofactor ($+0.5$ to $+0.7 \text{ V vs NHE}$) in order to be consistent with the properties of the catalyzed reaction. Iron complexes with nitrogen and carboxylate ligands such as iron(III)–EDTA and iron(III)–DTPA typically have much lower electrode potentials (ca. $+0.1 \text{ V vs NHE}$).⁴³ It is clear, however, from the accumulating crystallographic evidence regarding the lipoxygenase iron site that there is a lot of flexibility in the coordination geometry (Table 2). Protein dynamics may be a key component of the hydrogen tunneling mechanism.⁴⁴ The three-dimensional structures indicate that fluctuations in the relative positions of the iron atom and its ligands can indeed take place.

Experimental Section

Lipoxygenases were extracted from soybeans cv. Resnik and purified by ammonium sulfate fractionation and chromatofocusing.⁴⁵ Solutions of the enzymes in Tris HCl (0.1 M , $\text{pH } 7.0$) were stored at $4 \text{ }^\circ\text{C}$. Samples of the proteins were transferred into the appropriate buffers using dialysis and/or diafiltration using $50\,000 \text{ NMWCO}$ membranes. Cumene hydroperoxide was purified from an old bottle of cumene by chromatography on silica. Cumene and cumene hydroperoxide were

- (33) Ursby, T.; Adinolfi, B. S.; Al-Karadaghi, S.; De Vendittis, E.; Bocchini, V. *J. Mol. Biol.* **1999**, *286*, 189–205.
 (34) Nelson, M. J. *J. Am. Chem. Soc.* **1988**, *110*, 2985–2986.
 (35) Skrzypczak-Jankun, E.; Amzel, L. M.; Kroa, B. A.; Funk, M. O. *Proteins Struct. Funct. Genet.* **1997**, *29*, 15–31.
 (36) Wedekind, J. E.; Frey, P. A.; Rayment, I. *Biochemistry* **1995**, *34*, 11049–11061.
 (37) Geeganage, S.; Frey, P. A. *Biochemistry* **1999**, *38*, 13398–13406.
 (38) Kitajima, N.; Tamura, N.; Amagai, H.; Fukui, H.; Moro-oka, Y.; Mizutani, Y.; Kitagawa, T.; Mathur, R.; Heerwegh, K.; Reed, C. A.; Randall, C. R.; Que, L.; Tatsumi, K. *J. Am. Chem. Soc.* **1994**, *116*, 9071–9085.
 (39) Ogo, S.; Wada, S.; Watanabe, Y.; Iwase, M.; Wada, A.; Harata, M.; Jitsukawa, K.; Masuda, H.; Einaga, H. *Angew. Chem., Int. Ed. Engl.* **1998**, *37*, 2102–2104.
 (40) Goldsmith, C. R.; Jonas, R. T.; Stack, T. D. P. *J. Am. Chem. Soc.* **2001**, *124*, 83–96.
 (41) Kim, J.; Zang, Y.; Costas, M.; Harrison, R. G.; Wilkinson, E. C.; Que, L. *J. Biol. Inorg. Chem.* **2001**, *6*, 275–284.

- (42) Cha, Y.; Murray, C. J.; Klinman, J. P. *Science* **1989**, *243*, 1325–1330.
 (43) Engelmann, M. D.; Bobier, R. T.; Hiatt, T.; Cheng, I. F. *BioMetals* **2003**, *16*, 519–527.
 (44) Klinman, J. P. *Pure Appl. Chem.* **2003**, *75*, 601–608.
 (45) Funk, M. O.; Carroll, R. T.; Thompson, J. F.; Dunham, W. R. *Plant Physiol.* **1986**, *82*, 1139–1144.

batch eluted with hexane and collected as fractions in 5% acetone in hexane (v/v), respectively. Stock solutions of the hydroperoxide were prepared by weight in absolute methanol and stored at -80°C . The 13-HPOD was prepared from linoleic acid (Sigma) by the reaction catalyzed by lipoxygenase-1 at pH 9.2 and was purified by chromatography on silica.⁴⁶ Samples were prepared in absolute methanol and stored at -80°C . The concentration was determined by dilution in absolute methanol and UV-vis spectrophotometry using an ϵ value of 23 000 L/mol-cm.⁴⁷

Kinetic Measurements. The time course for the catalyzed reaction was obtained by following the formation of product, 13-HPOD, by the increase in absorbance at 234 nm at 25.0°C in a temperature-controlled Cary 3E spectrophotometer. Linoleic acid solutions were prepared in sodium borate buffer (0.1 M, pH 9.0). The substrate (3.00 mL) and appropriate dilutions of cumene hydroperoxide in methanol (0.060 mL) were transferred to a cuvette and temperature equilibrated with magnetic stirring. An aliquot of the enzyme (0.010 mL, $0.5\ \mu\text{M}$) was added to initiate the reaction, and the absorbance at 234 nm versus time was saved as a csv data file. The maximum slope as an approximation of the steady-state rate was obtained using an interactive plotting program in Excel.⁴⁸ Each determination was conducted three times consecutively, and the values were averaged. Each set of conditions was investigated at least three different times, and the values were averaged. The error represents the standard deviation found for a given set of conditions obtained on different occasions. Simulations of the maximum rate data were conducted with the interactive program DynaFit.⁴⁹ The kinetic mechanism derived by Schilstra et al. was used.¹⁶ The rate/dissociation constants employed in the simulations were $K_{\text{P}} = K_{\text{P}}^* = 12\ \mu\text{M}$, $K_{\text{S}} = K_{\text{S}}^* = 12\ \mu\text{M}$, $k_1 = 300\ \text{s}^{-1}$, $k_2 = 10^9\ \text{M}^{-1}\ \text{s}^{-1}$, $k_3 = 2300\ \text{s}^{-1}$, and $k_4 = 150\ \text{s}^{-1}$.

Preincubation of lipoxygenase-1 (1.00 mL, $0.5\ \mu\text{M}$) was carried out with varying concentrations of cumene hydroperoxide (0.02 mL in methanol) at 25°C in sodium borate buffer. An aliquot (0.010 mL) of the preincubation solution was added to 3.00 mL of temperature-equilibrated (25.0°C) substrate (linoleic acid, $100\ \mu\text{M}$, 2% methanol v/v) to initiate the reaction. The maximum slope was obtained for three consecutive determinations, and the values were averaged. The experiments were all replicated on separate occasions, and the values were averaged.

Isothermal Titration Calorimetry. Titrations were conducted in a MicroCal VP-ITC microcalorimeter. The enzyme (0.008 mM) was in the cell in Tris HCl (0.1 M, pH 8.5). The concentration of the cell solution was determined by absorbance at 280 nm using an ϵ value of 120 000 L/mol-cm.⁵⁰ The hydroperoxides were in the titration syringe (0.100 mM) in the same buffer. The concentration of cumene hydroperoxide solutions was determined by absorbance at 257 nm using an ϵ value of 190 L/mol-cm.⁵¹ The titrations consisted of 30 injections. A small heat of dilution contribution evident toward the end of each titration was subtracted from the data prior to fitting with Origin (one site). The experiments were carried out three times for both hydroperoxides. The reported error represents the standard deviation of three determinations on separate occasions.

EPR Spectroscopy. The 9 GHz spectra were obtained on frozen solutions in a Bruker model ESP 300E spectrometer with an Oxford Instruments model ITC4 cryostat operating at 25 K. Microwave power was selected to avoid modulation broadening, typically 5 mW with 1 mT modulation amplitude. The samples were prepared by placing the appropriate quantity of cumene hydroperoxide solution in methanol (1, 2, 5, and 10 times the amount of lipoxygenase-1) in an Eppendorf

tube. The methanol was removed using a stream of nitrogen. A sample of the enzyme (0.25 mL, $213.5\ \mu\text{M}$, 0.1 M Tris HCl pH 7.0) was added, and the contents were gently mixed. The samples were transferred to EPR tubes and frozen in liquid nitrogen.

Mass Spectrometry. Mass spectra were obtained at the Ohio State University Mass Spectrometry and Proteomics Facility of the Campus Chemical Instrument Center on a Micromass Q-ToF II High Resolution electrospray ionization mass spectrometer. The instrument was configured to simultaneously collect MS and MS/MS data on the effluent from a Vydac $2.1 \times 250\ \text{mm}$ C18 Mass Spec HPLC column in a Hewlett-Packard Series 1100 HPLC. The chromatography column was eluted at 0.1 mL/min with a 120 min linear gradient from 1% to 65% 0.1% formic acid in acetonitrile starting with 0.1% formic acid in water. Lipoxygenase-1 (0.4 mL, $38.4\ \mu\text{M}$) was added to a solution of cumene hydroperoxide ($2.27\ \mu\text{M}$, 9.6 mL) in 0.1 M Tris HCl pH 8.5, 2% methanol, (v/v). After 30 min at room temperature, the enzyme solution was transferred to 0.1 M ammonium bicarbonate by diafiltration using 50,000 NMWCO membranes. The final volume of each sample was 0.8 mL. The enzyme solutions were subjected to reduction, carboxamidomethylation, and trypsin digestion by closely following a published procedure.⁵²

X-ray Crystallography. Lipoxygenase-3 solutions were dialyzed against Tris HCl buffer (0.1 M, pH 7.0), concentrated to $10\ \text{mg mL}^{-1}$ and crystallized in a large batch technique by vapor diffusion in small concentric beakers cut to approximately 10 mm in height. The crystallization solution consisted of 600 μL of 20% PEG 8000 (w/v) in sodium citrate-phosphate buffer (0.05 M, pH 4.6), 100 μL of sodium phosphate buffer (0.1 M, pH 7.0), and 200 μL of deionized water. The solution was subsequently filtered through an ULTRAFREE-MC filter unit (0.45 μm) to remove any insoluble material. Microseeds were prepared by crushing available crystals in 20% PEG (w/v, 500 μL) using a pellet pestle mixer. The seed solution was diluted 1:100, and an aliquot (2–4 μL) was added to the crystallization solution. A small beaker (20 mm diameter \times 10 mm height) containing the crystallization solution was placed in a larger beaker (40 mm diameter \times 20 mm height) containing 5 mL of 20% PEG 8000 reservoir solution. The larger beaker was sealed with a glass plate and placed in an incubator at 23°C . Crystals formed in 24–72 h and grew to be 0.5 mm long with $0.05 \times 0.2\ \text{mm}$ cross-section dimensions.

Optically flawless crystals were transferred to a solution of cumene hydroperoxide prepared by combining 20 μL of a stock solution (0.375 M) in methanol with a solution of PEG 8000 (20%, w/v, 1 mL). Crystals were soaked for 12–24 h and subsequently equilibrated with 20% glycerol for cryoprotection. Glycerol was added incrementally over a period of 8 h, increasing the concentration gradually from 0.5% to 20%. A gradual increase in glycerol concentration prevented the lipoxygenase-3 crystals from going through a transition to a P lattice during flash-freezing as has been previously reported.²⁷

Crystals were flash-cooled for data collection under a nitrogen cryostream at 98 K. Diffraction data were collected with a Quantum 210 ADSC at the IMCA-CAT beamline 17-ID of the Advanced Photon Source at Argonne National Laboratory. Crystals diffracted to a resolution limit of 1.95 \AA with mosaicity values ranging from 0.9 to 1.4 \AA . All reflections were reduced using the DENZO/SCALEPACK crystallographic data-reduction package.⁵³ The unit cell parameters were $a = 111.001\ \text{\AA}$, $b = 136.901\ \text{\AA}$, $c = 61.512\ \text{\AA}$, and $\beta = 96.236^{\circ}$ with space group C2. The data set was 83% complete to 2.0 \AA resolution with an overall R_{merge} of 5.4%. The data collection statistics are provided in Table 3.

The structure of cumene hydroperoxide treated lipoxygenase-3 was determined by molecular replacement using the room-temperature structure of the 13-HPOD-lipoxygenase-3 complex (PDB 1IK3) as

(46) Funk, M. O.; Isaac, R.; Porter, N. A. *Lipids* **1976**, *11*, 113–117.

(47) Graff, G.; Anderson, L. A.; Jaques, L. W. *Anal. Biochem.* **1990**, *188*, 38–47.

(48) Brault, P. A. M.S. Thesis, University of Toledo, 2000.

(49) Kuzmic, P. *Anal. Biochem.* **1996**, *237*, 260–273.

(50) Draheim, J. E.; Carroll, R. T.; McNemar, T. B.; Dunham, W. R.; Sands, R. H.; Funk, M. O. *Arch. Biochem. Biophys.* **1989**, *269*, 208–218.

(51) Norrish, R. G.; Searby, M. H. *Proc. R. Soc. London* **1956**, *A237*, 464–.

(52) Stone, K. L.; Williams, K. R. *A Practical Guide to Protein and Peptide Purification for Microsequencing*, 2nd ed.; Academic Press: San Diego, 1993; Chapter 2.

(53) Otwinowski, Z.; Minor, W. *Methods Enzymol.* **1997**, *276*, 307–326.

Table 3. Data Collection and Space Group/Refinement Statistics for Cumene Hydroperoxide Treated Lipoxygenase-3 Crystals

beamline	APS IMCA-CAT Beamline 17-ID
detector	Quantum 210 ADSC
temperature (K)	98
wavelength (Å)	1.00
space group	C2
unit cell dimensions (Å), <i>b</i> (deg)	111.001, 136.901, 61.512, 96.236
no. of monomers in asymmetric unit	1
Matthews coefficient, V_M (Å ³ /Da)	2.4 (48.5%, v/v, solvent)
no. of images	178
approximate exposure time (s)	15
oscillation angle, $\Delta\phi$ (deg)	0.7
crystal to detector distance (mm)	200
resolution range (Å)	50–2.0
no. of observations	109 207
unique reflections	50 653
completeness (%)	83.0
mean $I/\sigma(I)$	15.9
Multiplicity	2.4
R_{sym} (%)	5.4
R -factor (50–2.0Å)	21.47
Free R -factor (50–2.0Å)	22.13
Average B -factor (Å ²)	32.7

^a The X-ray data were processed using the CCP4 package. Solvent content calculations were based on the expected solvent content of protein crystals.

starting coordinates for rigid body refinement with CNS.⁵⁴ All water molecules, heteromolecules (13-HPOD), and the iron atom were omitted, resulting in an initial R factor of 38.0% (R_{free} of 43.5%). Cryocooling resulted in an expected shrinkage of the unit cell dimensions. Simulated annealing followed by a cycle of positional and B -value refinement improved the R factor to 26.7% with R_{free} of 28.4%.

(54) Brunger, A. T.; Adams, P. D.; Clore, G. M.; Delano, W. L.; Gros, P.; Grosse-Kunstleve, R. W.; Jiang, J. S.; Kuszewski, J.; Pannu, N.; Read, R. J.; Rice, L. M.; Simonson, T.; Warren, G. L. *Acta Crystallogr., Sect. D* **1998**, *54*, 905–921.

The active site iron and the solvent structure were modeled and refined at this stage. $F_o - F_c$ and $2F_o - F_c$ electron density maps were calculated showing excellent density for the main chain and good density for the side chains. The Ramachandran plot performed with PROCHECK indicated that 84.8% of residues fell within the sterically most favored region with an additional 12.1% and 2.1% within the allowed and generously allowed regions, respectively.⁵⁵ Active site $F_o - F_c$ and omit $F_o - F_c$ maps were created, and a fifth ligand was modeled and refined. In addition, on the basis of mass spectrometry evidence, $F_o - F_c$ and omit $F_o - F_c$ maps were examined for evidence of side chain oxidation of Trp-519, Ser-564, Leu-565, and Val-566. Trp-519 showed very clear evidence for hydroxylation at the $C\beta$ position at electron density levels of 3σ . A similar hydroxylation site was found at the $C\beta$ position of Leu-565. The last stage of refinement included more B -value refinement and positional refinement with relaxation of bond length restraints for the hydroxylation sites. The B -values for the hydroxylation sites (occupancy = 1.0) at Trp-519 and Leu-565 refined to 30.6 and 33.0, respectively, compared with an average B -value for the structure of 32.7. The B -value for the iron-bound OH refined to 32.2 with a relaxed bond length of 2.05 Å. The final R factor for the resolution range, 50–2.0 Å, was 21.5% (R_{free} 22.1%).

Acknowledgment. This research received financial support from the National Institutes of Health (GM 62140). We are grateful to Zhenwei Lu for carrying out the alignments of the three-dimensional structures. We thank the staff members of the Industrial Macromolecular Crystallography Association Collaborative Access Team (IMCA-CAT) for their assistance with data collection.

JA0390855

(55) Laskowski, R. A.; MacArthur, M. W.; Moss, D. S.; Thornton, J. M. *J. Appl. Crystallogr.* **1993**, *26*, 283–291.